Research Paper

Journal of Vascular Research

J Vasc Res 2003;40:368–377
DOI: 10.1159/000072701

Received: February 3, 2003
Accepted after revision: April 18, 2003
Published online: July 29, 2003

CD34+ Blood Cells Accelerate Vascularization and Healing of Diabetic Mouse Skin Wounds

E. Sivan-Loukianova[a] O.A. Awad[a] V. Stepanovic[a] J. Bickenbach[b]
G.C. Schatteman[a]

Departments of [a]Exercise Science and [b]Anatomy and Cell Biology, University of Iowa, Iowa City, Iowa, USA

Key Words
Angiogenesis · Diabetes · Endothelial progenitor · Endothelium · Skin · Stem cell · Wound healing

Abstract
Diabetes is characterized by poor circulation and impaired angiogenesis, which appear to contribute to the frequent skin lesions and poor wound healing common in diabetic patients. Therapies to improve circulation commonly improve wound healing in diabetic patients. Administration of circulating CD34+ cells, cells that can function as endothelial cell progenitors, accelerates blood flow restoration to ischemic limbs of diabetic mice. We have investigated the potential of these cells to accelerate revascularization and healing in full-thickness skin wounds of hypoinsulinemic (streptozotocin-treated) diabetic mice. Wounds were injected with human CD34+ or CD34– peripheral blood mononuclear cells or no cells, and analyzed for vascularity and healing at various times thereafter. Treatment with CD34+ enriched cells decreased wound size by 4 days after treatment, accelerated epidermal healing, and rapidly and dramatically accelerated revascularization of the wounds compared to controls. Initially increased vascularization was mediated principally by an increase in vessel diameter, but later, both an increase in vascular size and number were observed. These findings indicate that blood-derived progenitors may have therapeutic potential in the treatment of skin lesions in the setting of diabetes, and give insights into how bone marrow cells exert their effects on neovascularization.

Supported by grants from the National Institutes of Health via a pilot grant from the NIH DK25295 Diabetes and Endocrinology Research Center (G.C.S.) and DK59223 (G.C.S. and J.B.).

Introduction

Skin lesions are a severe and frequent complication of diabetes. Among these, ulcers of the lower limbs cost the US Medicare system USD 1.5 billion in 1995 [9]. There are many causes of diabetic skin wounds and ulcers including neuropathy, trauma, and ischemia, but whatever the etiology, their healing in diabetic patients is compromised [13]. Non-healing ulcers are the most common cause of amputation, and in one study, diabetic ulcers were the cause of 84% of amputations among diabetic

KARGER
Fax + 41 61 306 12 34
E-Mail karger@karger.ch
www.karger.com

1018–1172/03/0404–0368$19.50/0

Accessible online at:
www.karger.com/jvr

Assist. Prof. Gina C. Schatteman
Exercise Science FH406
University of Iowa
Iowa City, IA 52242-1111 (USA)
Tel. +1 319 335 9486, Fax +1 319 335 6966, E-Mail gina-schatteman@uiowa.edu

patients [16, 17]. The microvasculature of the diabetic skin exhibits both structural and functional abnormalities that contribute to impaired wound healing and ulcer formation. One of the functional manifestations of these vascular abnormalities is low cutaneous blood flow, which is probably the greatest risk factor for amputation [17]. Additionally, there is a reduction in sensory innervation in the skin of diabetic patients, and this reduction inhibits normal tissue repair [4, 8, 11, 15, 20].

While circulatory abnormalities and neuropathy contribute to delayed wound healing and chronic wounds in diabetic patients, precisely how these factors impact on the wounds is unclear [1, 3]. Does neuropathy lead to angiopathy, vice versa, or are the two unrelated? Despite our lack of understanding, a number of studies indicate that improving one tends to improve the other [2, 6, 19]. In addition to macro- and microcirculatory problems, angiogenesis is impaired in diabetic compared to non-diabetic patients, and this angiogenic delay may also contribute to poor wound healing [7, 21, 23].

Numerous studies demonstrate that a subset of hematopoietic cells can function as adult stem cells, and it appears that leukocytes expressing the cell surface antigen CD34+ are enriched for these stem cells. Blood-derived stem cells are capable of differentiating into a variety of cell types, including endothelial cells [5, 22]. However, the ability of adult blood-derived cells to function as endothelial cell progenitors appears to be reduced by diabetes. In vitro, stem cells derived from type I diabetic patients produced significantly fewer endothelial cells per milliliter of blood than did cells from non-diabetic controls. Also, whereas grafted exogenous stem cells from non-diabetic humans had no effect on the restoration of blood flow to an ischemic limb in non-diabetic mice, the same cells profoundly accelerated blood flow restoration in diabetic mice, suggesting that endogenous cells are functionally deficient [18].

Since exogenous CD34+ peripheral blood mononuclear cell (PBMC) administration has a rapid and significant effect on revascularization of ischemic limbs in streptozotocin-treated (diabetic) mice, we hypothesized that these cells could also accelerate revascularization of skin wounds, which might in turn improve wound healing in diabetic mice. As a corollary we hypothesized that CD34– PBMCs would not exhibit these properties since they failed to accelerate flow restoration in the ischemic limb. A finding that CD34+ PBMCs could improve vascularization of skin wounds would strongly suggest that exogenous CD34+ PBMCs may have therapeutic potential in the treatment of skin lesions in the setting of diabetes.

Methods

Animal Procedures

All procedures were performed according to the University of Iowa Animal Care and Use Committee guidelines following the principles of animal care. To induce diabetes, 8- to 10-week-old male nude mice (NU/J Hfh11^{nu} from Jackson Laboratories, Bar Harbor, Me., USA) were treated with low-dose streptozotocin (Sigma, St. Louis, Mo., USA). Mice were injected intraperitoneally with 43 mg/kg streptozotocin in 0.05 *M* Na citrate, pH 4.5, daily for 5 days [12]. Three days after the final injection, blood glucose levels were measured using an Accu-Chek glucometer (Roche, Indianapolis, Ind., USA). Mice with blood glucose levels >250 mg/dl and polyuria as assessed by wet cage bedding were considered to have diabetes. Serum glucose levels in control nude mice typically average 120 mg/dl [18].

Three to four weeks after induction of diabetes, mice were anesthetized by intraperitoneal injection of 80 μg ketamine plus 10 μg xylazine/g and the skin cleaned with povidone-iodine. Bilateral full-thickness skin wounds were created on the dorso-rostral back using a sterile 4-mm biopsy punch. Three days later, mice were anesthetized, and freshly isolated human CD34+ enriched PBMCs from 45 ml of human peripheral blood (3–6 $\times 10^5$ cells) in 25 μl 0.9% NaCl were injected under each wound bed. In some experiments, the same number of CD34– PBMCs, i.e. PBMCs depleted of CD34+ cells, were injected. Control mice were injected with 0.9% NaCl. Nude mice were used to minimize possible host-versus-graft immune responses to the transplanted human cells.

Isolation and Labeling of CD34+ and CD34– PBMCs

Human blood was collected from healthy volunteer donors after obtaining informed consent and according to protocols approved by the University of Iowa Institutional Review Board. 90 ml of blood were collected into 10 ml 0.13 *M* sodium citrate as anticoagulant and used immediately. Blood was diluted with 0.5 volumes PBS/AC (1.1 m*M* KH_2PO_4, 3 m*M* Na_2HPO_4, 0.9% NaCl, 0.13 M sodium citrate, pH 7.2), and PBMCs were fractionated from red blood cells by centrifugation over Histopaque 1077. PBMCs were washed thrice in PBS/AC with 2% bovine serum albumin (BSA). CD34+ enriched PBMCs were collected using CD34-antibody-coated magnetic beads then detached from the beads by enzymatic digestion of the bead-antibody linkage according to the manufacturer's (Dynal, Lake Success, N.Y., USA) instructions and as previously described [18]. The remaining PBMCs served as CD34– control cells.

Tissue Preparation and Immunostaining

Animals were sacrificed on days 7, 14 and 21 after wounding. Wound beds surrounded by a margin of normal skin and the underlying muscle layer were harvested and fixed 4 h in 100% methanol at room temperature, then processed through 100% ethanol, xylenes and paraffin embedded. Wounds were serially sectioned (7 μm) perpendicular to the wound surface rostral to caudally. A total of eight wounds (from 4–6 different mice) in each group were analyzed. The number of sections analyzed ranged from 15–22 per wound depending on the size of the wound.

Every tenth section was stained with hematoxylin and eosin for wound analysis. To visualize blood vessels, the adjacent sections were deparaffinized and immunolabeled with anti-CD31 (BD Pharmingen, San Diego, Calif., USA) or anti-von Willebrand factor (vWF; DAKO, Carpenteria, Calif., USA). For CD31 staining, sections were treated for 3 min at 37°C with 100 mg/ml proteinase K

Table 1. Formulas for computing wound and vascular parameters

Parameter	Formula	Definitions
Wound area	$A_W = A_E + A_D$ (mm^2)	A_E = epidermal area A_D = dermal area
Wound volume	$V_W = 0.070\ mm \cdot \Sigma_{n = 2\ to\ N}(A_n + A_{(n-1)})/2$	A = area of the wound N = total number of sections/10 (sections are 7 μm thick)
Vascular area density	$V_D = 100 \cdot \Sigma_{n = 1\ to\ N}[(A_{BV})_{10n}/(A_W)_{10n}]/N$	A_W = area of wound A_{BV} = area of the blood vessels N = total number of sections/10
Total vascular volume	$V_{BV} = V_D \cdot V_W$ (mm^3)	N_{BV} = number of blood vessels
Vascular index	$V_I = \Sigma_{n = 1\ to\ N}[(N_{BV})_{10n}/(A_W)_{10n}]/N$	A_W = area of wound N = total number of sections/10

(BD Pharmingen), blocked in 2% BSA in PBS, incubated for 1 h at 37°C in 2.5 μg/ml anti-CD31, then 0.75 μg/ml biotinylated anti-rat IgG, and next with 1:200 alkaline phosphatase-streptavidin complex (Vector, Burlingame, Calif., USA) for 1 h. Immunolabeling was visualized with Vector Red (Vector). vWF staining was done similarly except that sections were treated 2 min with 10% acetic acid in PBS before proteinase K digestion, incubated in 4 μg/ml anti-vWF 1 h at room temperature and overnight at 4°C followed by 7.5 μg/ml biotinylated anti-rabbit IgG (Vector), reacted with 1.25 μ/ml streptavidin-horseradish peroxidase 1 h at room temperature, and treated with 0.08 μg/ml diaminobenzidene and 0.03% H_2O_2. Non-immune IgG of the appropriate species at the same concentrations served as control. Immunolabeled sections were stained with hematoxylin.

To investigate if CD34+ enriched PBMCs themselves contribute to the endothelium of the wound neovasculature, sections from day-14 CD34+ cell-treated wounds were co-immunolabeled with 2.5 μg/ml rhodamine *Ulex europaeus* I lectin (Vector) to detect human and 5 μg/ml fluorescein *Bandeiraea simplicifolia* lectin B_4 (Vector) to detect mouse endothelial cells. After deparaffinization and blocking in 2% BSA in PBS, sections were incubated 2 h at room temperature in each lectin, sequentially.

Wound Analysis

Images of every tenth hematoxylin- and eosin-stained section were captured digitally (Nikon E600 microscope and DXM1600 camera). The periphery of the wound epidermis and dermis were each traced digitally to determine the area of each in the wound using Metavue software (Universal Imaging, Downington, Pa., USA). The total wound area in each section was computed as the sum of the epidermis and dermis to avoid errors associated with artifactual separation of epidermis and dermis, except in sections from day 7 wounds, where the entire wound was traced since not all wounds were closed. Lateral wound boundaries were determined by the presence of intact hair follicles and organized epidermis and dermis as compared to a lack of hair follicles, altered epidermal/dermal organization, and disorganization of collagen fibers within the wound (fig. 1). For vascular measurements, anti-CD31 immunolabeled blood vessels in the adjacent section (that is, every tenth section) were traced. From these measurements the total wound volume, percent epidermis (epidermal area per total wound area), vascular area density (blood vessel area per wound area), total blood vessel volume in the wound, and the vessel index (number of blood vessels per wound area) were determined directly using Metavue software or calculated using the formulas in table 1. Additionally, the size distribution of the luminal area of vessels in the histological sections was determined. Vessels were assigned to one of five groups, ≤ 5, 5–11, 11–16, 16–21, and $>21 \times 10^{-5}$ mm^2, according to size. The percentage of vessels partitioned into each group was computed.

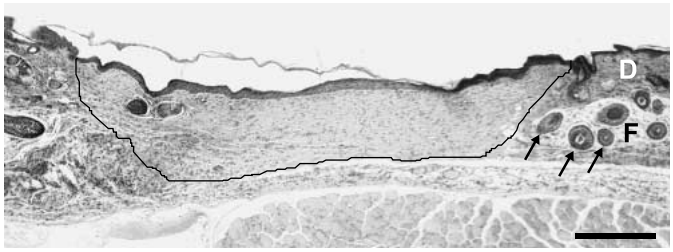

Fig. 1. Delineation of the wound bed: HE-stained section of a skin wound in a control mouse 14 days after wounding. Black line indicates area included in the measurement of the wound bed. Note the presence of hair follicles (arrows), thinner organized dermis, and clear delineation between dermis (D) and subcutaneous fat layer (F) in adjacent tissue. Bar = 1 mm.

Eight wounds from 4–6 mice in each group were analyzed. Data were compared between groups (time and treatment) using two-factor factorial ANOVA with $p < 0.05$ considered statistically significant. Post-hoc analyses were performed using Tukey's tests. Data were analyzed in two ways. First, each wound was considered an independent measure. Second, if two wounds were derived from the same animal, the data from the two wounds were averaged and taken as a single independent measure. Both analyses yielded similar results.

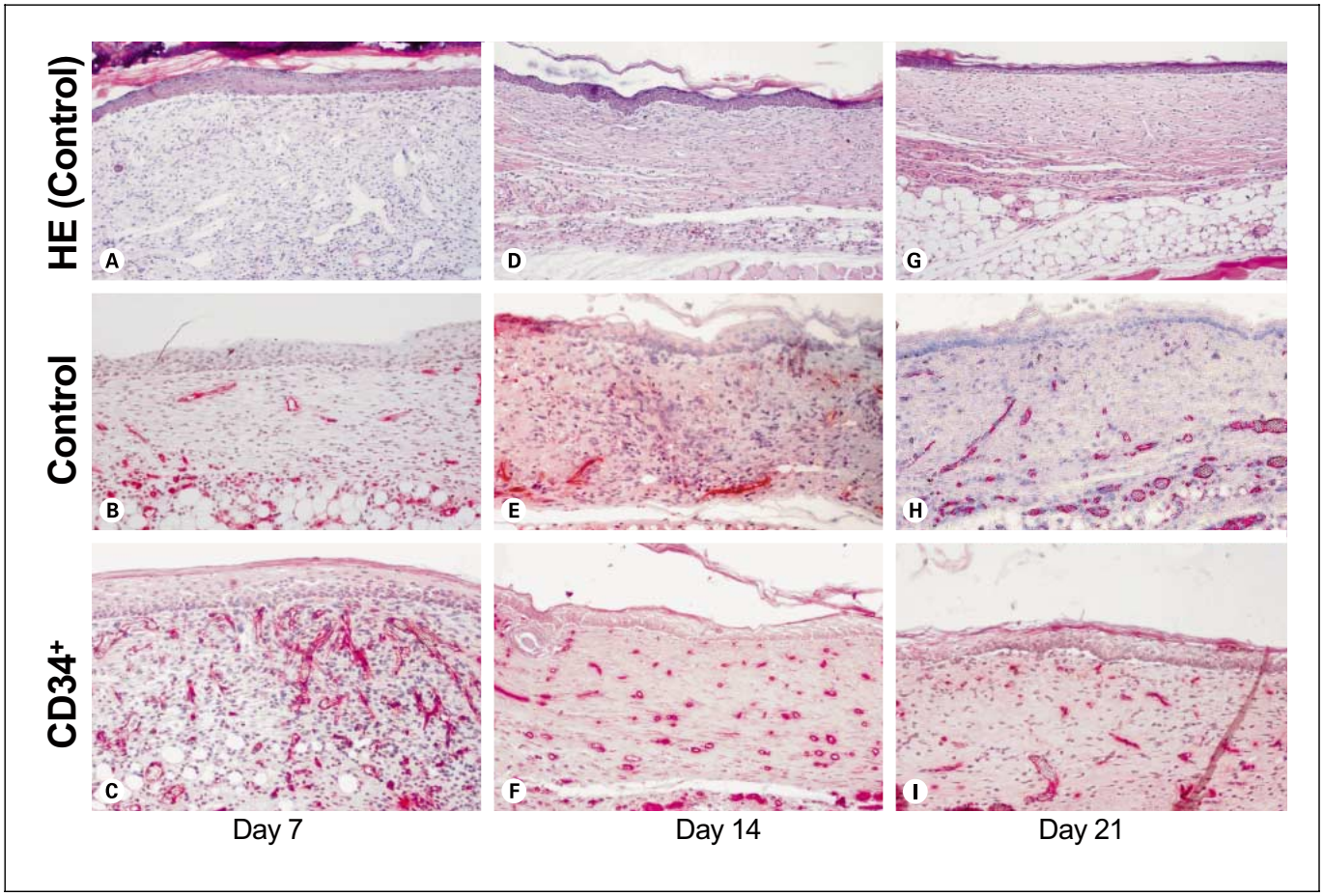

Fig. 2. Histology and CD31 immunolabeling. 7-μm HE-stained paraffin sections of skin 7 (**A**–**C**), 14 (**D**–**F**) and 21 days (**G**–**I**) after wounding. Some sections (**B**, **C**, **E**, **F**, **H**, **I**) were immunolabeled with anti-CD31 antibodies and visualized with a Vector Red (bright red substrate) to delineate blood vessels. In the control wounds, hyperplastic epidermis at 7 days (**A**) gradually decreases in thickness over time (**D**, **G**). Decreased CD31 immunoreactivity is apparent in 7- (**B**) and 14-day (**E**) control wounds compared to CD34+ cell-treated 7- (**C**) and 14-day (**F**) wounds. Vascularity in the dermis, as indicated by CD31 labeling, is similar in both control (**H**) and treated (**I**) wounds at 21 days. Bar = 400 (**A**, **D**, **G**) and 200 μm (**B**, **C**, **E**, **F**, **H**, **I**).

Results

Wound Morphology

Skin wound healing is delayed by diabetes and this is thought to be in part due to delayed revascularization [18]. Intramuscular injection of blood-derived CD34+ cell-enriched PBMCs accelerates revascularization of ischemic limbs in diabetic mice [18]. We therefore reasoned that CD34+ PBMCs may hasten wound healing in diabetic mice by accelerating revascularization of the wound. To investigate this, bilateral full-thickness punch biopsies were performed on the backs of T-cell-deficient nude diabetic mice. Three days later just prior to the start of wound revascularization, vehicle or human CD34+ PBMCs were injected under each wound. Wounds were subsequently harvested 7, 14, or 21 days after wounding, and hematoxylin- and eosin-stained tissue sections were examined. Both treated and untreated 7-day wounds were closed or almost closed and revascularization had begun, but a significant inflammatory reaction could be seen in the wounds in hematoxylin- and eosin-stained histological sections (fig. 2A). There was no correlation between the extent of inflammation and cell treatment. By 14 days revascularization was well advanced, little if any inflammation was present, and reorganization of collagen had begun (fig. 2D). At 21 days, wound tissue was well vascu-

larized, and epidermal thickness was returning to normal, but collagen reorganization remained incomplete (fig. 2G).

Morphometry

Every tenth section of each wound was hematoxylin and eosin stained, and the adjacent sections were immunolabeled with anti-CD31 which labels endothelial cells [14] (fig. 2). Additional sections were immunolabeled with anti-vWF, another endothelial cell antigen [10]. Comparison of adjacent sections labeled with the two antibodies showed indistinguishable patterns of labeling (data not shown). Because anti-CD31 labeling was brighter, this antibody was used for all analyses.

Epidermal and dermal areas of the wounds were determined by digitally analyzing images of hematoxylin- and eosin-stained slides. Immunolabeled sections were similarly imaged and the lumina of labeled vessels digitally traced to determine the area and number of vessels in each section. Mean vascular area density (area of blood vessels per area of wound), vessel index (mean number of vessels per unit area), wound volume and total vascular volume were calculated using the formulas in table 1.

CD34+ PBMCs Accelerate Wound Vascularization

Treatment with CD34+ PBMCs resulted in significant differences in vascular area density and total vascular volume in the wounds during the period examined. By 7 days after wounding (i.e. 4 days after treatment), vascular area density in the wound was 1.6-fold greater in CD34+ PBMC-injected wounds than in vehicle-treated wounds, and there was an increase in total vascular volume (fig. 2B, C, 3A, B). Fourteen days after wounding, vascular area density and total vascular volume in CD34+ PBMC-treated wounds were both 2.7-fold greater than that of vehicle-treated wounds (fig. 2E, F, 3A, B). Thus, during the period from 7 to 14 days after wounding, vascular area density increased from 4.0 to 5.4% in CD34+ cell-treated mice but decreased from 2.5 to 2.0% in vehicle control mice (fig. 3A). Additionally, whereas total vascular volume did not change significantly in CD34+ PBMC-treated wounds, it decreased more than 2-fold in control wounds (fig. 3B). Twenty-one days after wounding, the vascular area density and total vascular volume were similar in all mice, as a result of a decline in CD34+ cell-treated mice and an increase in control mice (fig. 2H, I, 3A, B).

To determine if the observed vascular area density improvements were specific to CD34+ enriched PBMCs, an additional group of mice was injected as above with CD34– PBMCs, i.e. PBMCs depleted of CD34+ PBMCs. Examination of wounds 14 days after injection showed no increase in vascular area density in the wounds treated with CD34– PBMC relative to vehicle controls (fig. 3C).

We next investigated the mechanism through which vascular area density increased, i.e. via an increase in the number or size of vessels in the wound. For this purpose, a frequency distribution of wound vessel size was plotted. Seven days after wounding, the CD34+ PBMC-induced increase in vascular area density was not accompanied by a significant increase in the vessel index (i.e. number of vessels per wound area; fig. 4A), but the frequency distribution in CD34+ PBMC-treated wounds was shifted to a larger vessel size relative to controls (fig. 5A). Fourteen days after wounding, the vessel index increased with CD34+ PBMC treatment (fig. 4A), and the frequency distribution remained shifted to larger vessels relative to controls (fig. 5B). By 21 days after wounding, the vessel index (fig. 4A) and the frequency distribution were similar in both groups (fig. 5C).

We again tested if the changes in the vasculature were specific to CD34+ enriched PBMCs. Surprisingly, injection of CD34– PBMCs also increased the vascular index, although not as much as CD34+ PBMCs (fig. 4B). However, there was a dramatic shift in the vessels size distribution to small vessels in these wounds compared to vehicle-treated controls (fig. 5D).

Several studies suggest that CD34+ PBMCs can differentiate into endothelial cells in vivo. Thus, at least two mechanisms are possible for the observed increase in vascularity in the wounds. The exogenous cells could be undergoing a vasculogenic transformation to form new vessels or incorporating into newly forming mouse vessels. Alternatively, the injected cells could be inducing endogenous cells to vascularize the wound. To differentiate between these possibilities, we labeled endothelial cells in sections of CD34+ PBMC-treated 14-day wounds. Rhodamine-conjugated Ulex lectin (which labels human but not mouse cells) and FITC-conjugated $BSLB_4$ lectin (which labels mouse but not human cells) were used to distinguish exogenous human cells from endogenous mouse cells. Examination of sections revealed rhodamine-labeled cells that appeared to be in the endothelial cell layer of blood vessels, but this was a relatively rare event. When present, they tended to be clustered in several vessels in a small area (data not shown).

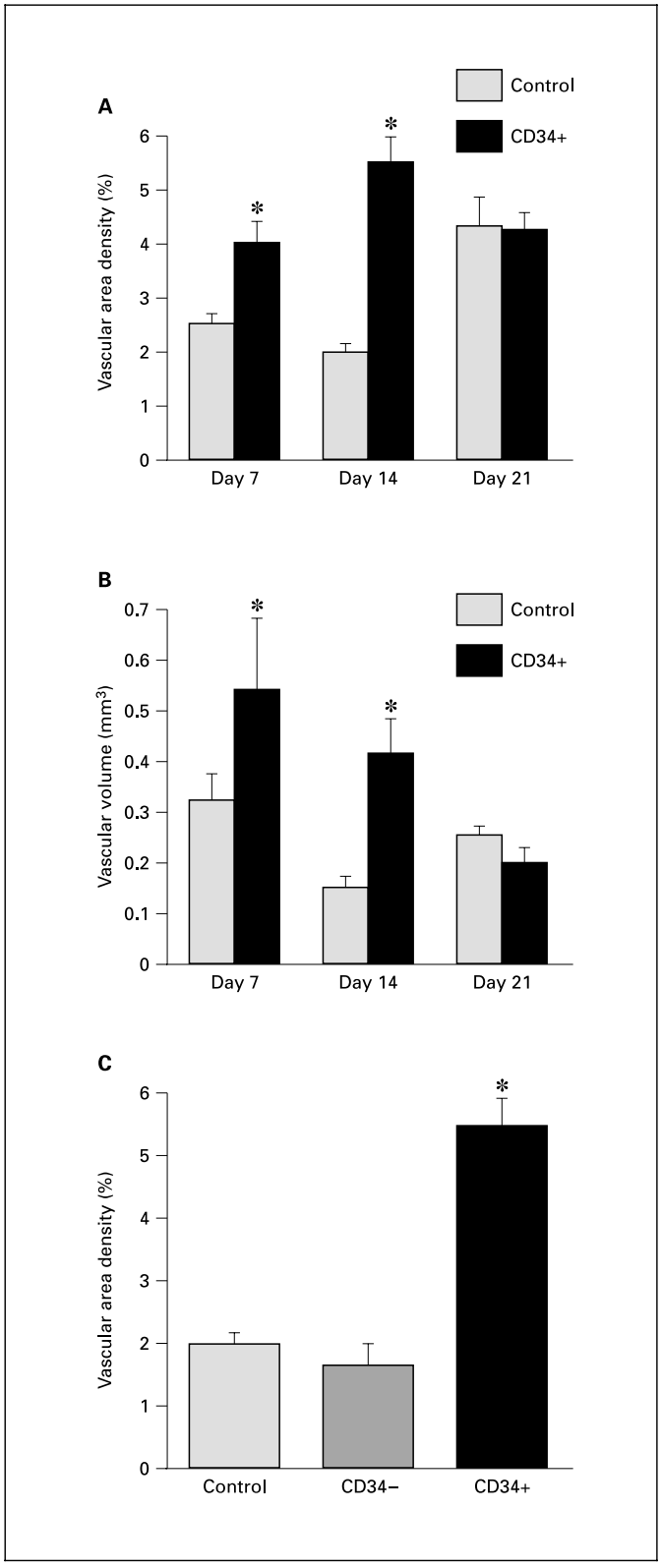

3

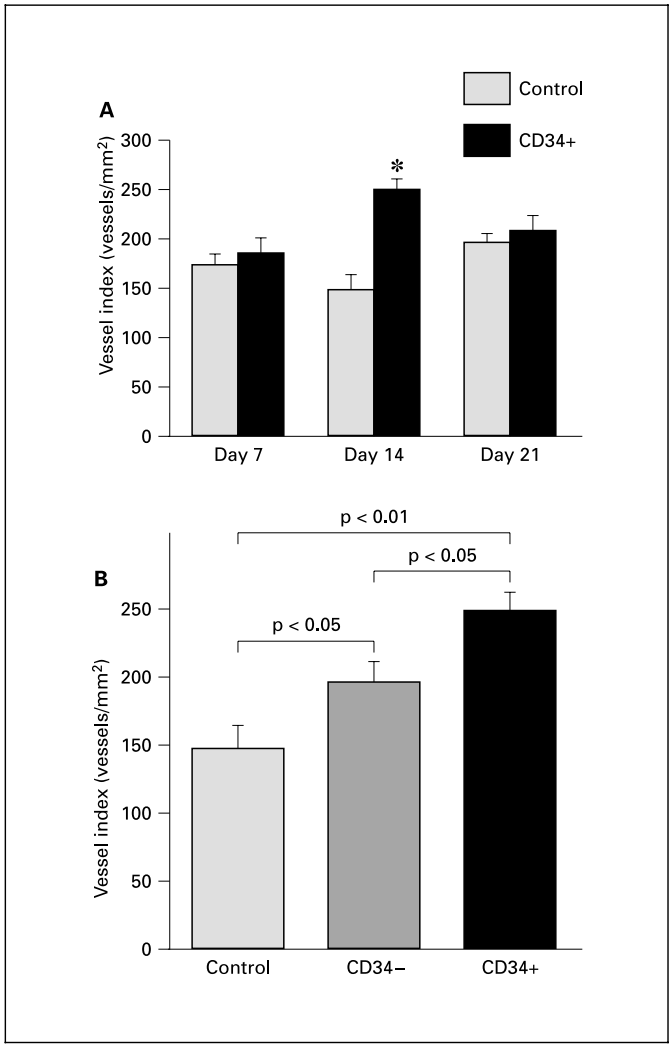

4

Fig. 3. Wound vascularization assessed by morphometric analysis of 7-μm anti-CD31-immunolabeled skin wound sections (**A**, **B**) of controls or wounds treated with CD34+ enriched PBMCs harvested 7, 14, and 21 days after wounding. **A** Vascular area density expressed as percent mean area of vascular lumina per wound area. **B** Total vascular volume within the wound. **C** Vascular area density in control wounds and wounds injected with CD34– or CD34+ PBMC harvested 14 days after wounding. * $p < 0.05$ vs. control on the same day.

Fig. 4. Vessel index assessed by morphometric analysis of 7-μm sections of anti-CD31-immunolabeled control or treated skin wounds. Vessel index is expressed as the number of blood vessels per area of wound. **A** Index in control or CD34+ PBMC-treated wounds harvested 7, 14, and 21 days after wounding. * $p < 0.05$ vs. control on the same day. **B** Index in wounds treated with CD34– or CD34+ PBMC or control wounds harvested 14 days after wounding.

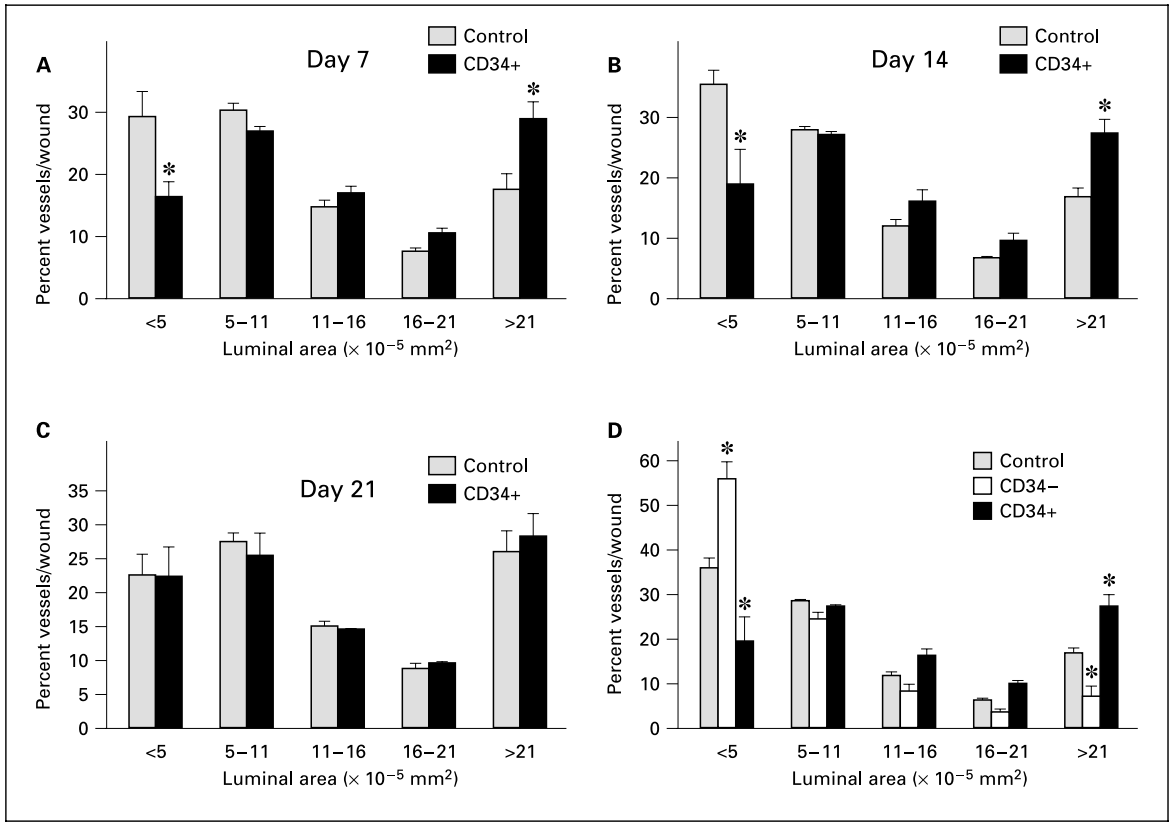

Fig. 5. Blood vessel size distribution determined by morphometric analysis of anti-CD31 immunolabeled 7-μm sections of skin wounds. Vessels were grouped according to luminal areas as indicated. **A**–**C** Vessel size analysis from control and CD34+ PBMC-treated wounds harvested 7 (**A**), 14 (**B**), or 21 (**C**) days after wounding. **D** Vessel size analysis from wounds treated with CD34– or CD34+ PBMC and control wounds harvested 14 days after wounding. * $p < 0.05$ vs. control of the same size range.

Effects of CD34+ PBMCs on Wound Healing

To determine if the increase in vascularity translated to improved skin wound healing, we compared total wound volume and epidermal thickness between CD34+ PBMC- and vehicle-treated wounds. At 7 days, only 3 days after treatment, average wound volume decreased by more than 30% in CD34+ PBMC-treated wounds relative to controls (fig. 6A). At both 14 and 21 days after wounding, there was no statistically significant difference in wound volume between the two groups (fig. 6A).

Epidermal healing is characterized by a re-epithelialization process that involves three phases. Initially, the wound is covered by a thin layer of epidermal cells, subsequently, the epidermis is hyperplastic, and finally the epidermis returns approximately to its pre-wounding thickness. We attempted to compare epidermal thickness in the control and CD34+ PBMC-treated wounds by measuring the area of the wound and dividing it by the length of the wound. However, interobserver measurements of length were not consistent, and the resulting estimated average epidermal thicknesses were extremely variable from section to section and among wounds in a group.

To circumvent this problem, we used instead an indirect means to estimate epidermal thickness. The ratio of the epidermal area to wound area was computed for each section. This ratio of measurements was highly reproducible and led to small standard errors within each group. At 14 days, when the epidermis is still hyperplastic, the ratio of epidermal area to wound area was greater in CD34+ PBMC-treated than in control wounds ($p < 0.05$), suggesting that the epidermis was thicker in treated wounds (fig. 6B). In contrast, at 21 days, this ratio was significantly decreased ($p < 0.05$) in CD34+ PBMC-treated than in control wounds (fig. 6B). Moreover, while this estimate of

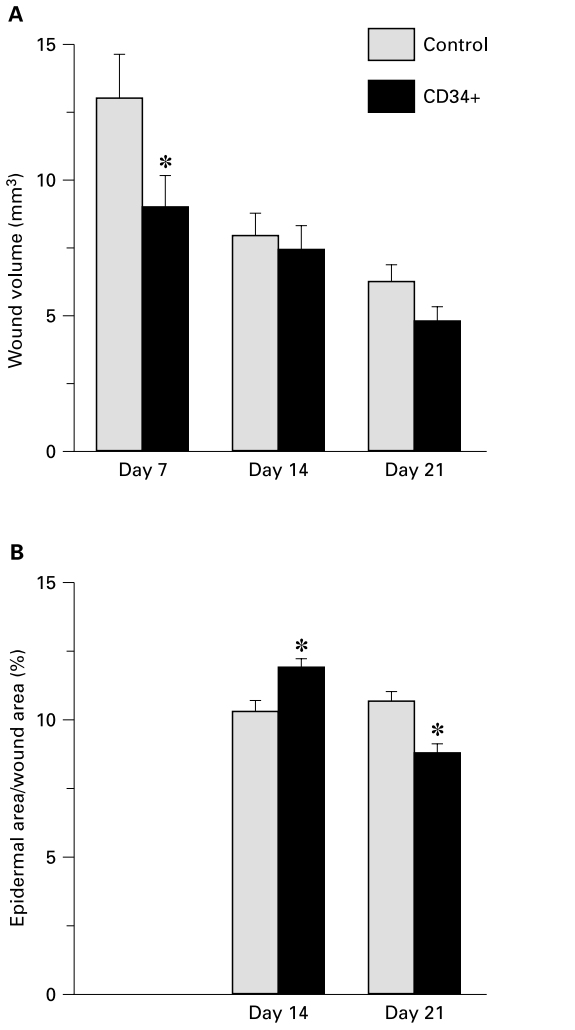

Fig. 6. Quantitation of wound healing. **A** Total wound volume in control and CD34+ cell-treated wounds 7, 14, and 21 days after wounding estimated by measuring the wound area in every tenth histological section of the entire wound and interpolation. *$p < 0.05$ vs. control of the same day. **B** Mean ratio of epidermal area to wound area per histological section (%). * $p < 0.05$ vs. control of the same day.

epidermal thickness did not change in control mice between 14 and 21 days, the ratio decreased significantly in this time period in CD34+ PBMC-treated wounds, suggesting that epidermal hypertrophy was receding in the treated but not control wounds (fig. 6B). Because not all wounds were completely epithelialized on 7 day, this ratio was not computed for the early time point.

Discussion

Impaired angiogenesis is a clinically significant problem in diabetic patients, and clinical trials indicate that therapies designed to improve vascularization can improve outcomes in patients with severe skin wounds and diabetic ulcers. Previously we demonstrated that injection of CD34+ enriched PBMCs into the ischemic limbs of diabetic mice could rapidly and significantly improve blood flow to the limbs [18]. In this study, we tested the potential of these same cells to improve vascularization of skin wounds in a mouse model of diabetes. Our data indicate that, compared to the controls, treatment with PBMCs enriched for CD34+ cells dramatically enhances revascularization of the wound by at least 7 days after wounding, i.e. just 4 days after injection of cells. Furthermore, this property is specific for this population of cells, as CD34– cells did not induce a similar effect.

In the initial 7-day wound healing period, the vascular index is similar in control and treated wounds (fig. 4A). Nevertheless, there are dramatic differences in both vascular volume and vascular area density between control and treated mice (fig. 3A, B). This difference can be attributed to a shift toward larger vessel luminal diameter in the treated wounds compared to controls (fig. 5A), indicative of either a vascular remodeling-like process in CD34+ cell-injected wounds or perhaps vasodilation.

Differences in vascularity in the two groups remain at 14 days, though the underlying mechanism changes. In the period from 7 to 14 days, there is an increase in the vascular index in treated mice (fig. 4A), an indication that increased neovascularization is occurring within the treated wound. Despite active neovascularization which would be expected to increase the proportion of small vessels, the vessel size distribution remains unchanged (fig. 5B), suggesting vascular remodeling or vasodilation. The latter seems unlikely, however, since CD34– PBMCs induce no analogous effect, and inflammatory responses in all groups are similar. Not surprisingly, the additional vascular growth during this week leads to increased vascular area density (fig. 3A), although total vascular volume is essentially unchanged (fig. 3B) due to a reduction in wound size. In contrast, the vessel index does not change significantly in control wounds between 7 and 14 days (fig. 4A), indicating little or no new blood vessel growth or a compensatory vessel loss. Moreover, small decreases in vascular area density and vascular index as well as a slight shift to decreased luminal size all contribute to a >50% decrease in total vascular volume in controls during this period (fig. 3B). Thus, it appears that not only is little or

no new vessel growth occurring in control wounds, there may also be selective loss of larger vessels.

Since section orientation affects both the vessel index and size distribution (but not the vascular area density), care was taken in orienting wounds with respect to the epidermal surface. For consistency, wounds were also oriented with respect to the anterior posterior axis, although skin vasculature is isotropic in the two planes perpendicular to the epidermal surface. Given these considerations and a sample size of eight wounds per group, it is unlikely that the observed effects are attributable to orientation artifacts. Moreover, as our standard error bars indicate, there was little or no overlap between groups, suggesting that differences were not due to a few misoriented wounds. In addition, while we cannot rule out the possibility that CD34+ PBMC injection induces vessel tortuosity, which would increase the vessel index, our histological data do not support this interpretation. There is no obvious tortuosity or difference in the shape of vessels in controls versus cell-treated mice other than size (fig. 2).

By 21 days, vascular parameters are similar in both groups. This appears to be due both to accelerated vascular growth in untreated wounds and a loss of vessels in CD34+ PBMC-treated wounds. In control wounds vascular index, volume, and density all increase during this period and there is a dramatic shift from small luminal size to larger vessels. In contrast, in CD34+ PBMC-treated wounds, vascular area density, index, and total volume decrease, and vessels size shifts to smaller luminal area.

Our data clearly demonstrate that CD34+ enriched PBMC-treated wounds are significantly more vascularized than wounds injected with CD34– PBMC or vehicle during the early stages of wound healing. Previous studies argued against a role for CD34– PBMC in increasing vascular area density or improving blood flow in the wounds compared to untreated controls, and our data are consistent with this. However, there do seem to be more vessels of smaller caliber in wounds treated with CD34– PBMC. Perhaps CD34– PBMC can induce vascular growth but in some way inhibit vessel maturation.

The increase in vascularization following CD34+ PBMC treatment correlates with a rapid (occurring within 4 days of treatment) >30% reduction in wound volume. This rapid early healing and/or the persistently increased vascularization in CD34+ PBMC-treated wounds may contribute to an apparent acceleration of epidermal remodeling. Since formation of a stable epidermis in chronic wounds of diabetics is problematic, this improvement could be significant, and could mean the difference between a skin wound that heals and one that becomes chronic. Thus, the observed changes in wound healing may prove meaningful in humans. More importantly, improved perfusion and/or blood flow could prevent loss of tissue to gangrene. Thus, our data indicate that CD34+ PBMC treatment to promote revascularization of diabetic skin wounds could improve wound healing, and this is being investigated further in a different model system.

Acknowledgments

The authors would like to thank Drs. Robert Tomanek and Martine Dunnwald for useful discussions and Kyce Brown for performing statistical analyses.

References

1 Adler AI, Neil HA, Manley SE, Holman RR, Turner RC: Hyperglycemia and hyperinsulinemia at diagnosis of diabetes and their association with subsequent cardiovascular disease in the United Kingdom prospective diabetes study (UKPDS 47). Am Heart J 1999;138: S353–S359.
2 Akbari CM, Gibbons GW, Habershaw GM, LoGerfo FW, Veves A: The effect of arterial reconstruction on the natural history of diabetic neuropathy. Arch Surg 1997;132:148–152.
3 Ansel JC, Armstrong CA, Song I, Quinlan KL, Olerud JE, Caughman SW, Bunnett NW: Interactions of the skin and nervous system. J Invest Dermatol Symp Proc 1997;2:23–26.
4 Aronin N, Leeman SE, Clements RS Jr: Diminished flare response in neuropathic diabetic patients. Comparison of effects of substance P, histamine, and capsaicin. Diabetes 1987;36: 1139–1143.
5 Asahara T, Murohara T, Sullivan A, Silver M, van der Zee R, Li T, Witzenbichler B, Schatteman G, Isner JM: Isolation of putative progenitor endothelial cells for angiogenesis. Science 1997;275:964–967.
6 Cameron NE, Cotter MA: Metabolic and vascular factors in the pathogenesis of diabetic neuropathy. Diabetes 1997;46(suppl 2):S31–S37.
7 Colville-Nash PR, Willoughby DA: Growth factors in angiogenesis: Current interest and therapeutic potential. Mol Med Today 1997;3: 14–23.
8 Haegerstrand A, Dalsgaard CJ, Jonzon B, Larsson O, Nilsson J: Calcitonin gene-related peptide stimulates proliferation of human endothelial cells. Proc Natl Acad Sci USA 1990;87: 3299–3303.
9 Harrington C, Zagari MJ, Corea J, Klitenic J: A cost analysis of diabetic lower-extremity ulcers. Diabetes Care 2000;23:1333–1338.
10 Jaffe EA, Nachman RL, Becker CG, Minick CR: Culture of human endothelial cells derived from umbilical veins. Identification by morphologic and immunologic criteria. J Clin Invest 1973;52:2745–2756.

11 Kennedy WR, Wendelschafer-Crabb G: Utility of skin biopsy in diabetic neuropathy. Semin Neurol 1996;16:163–171.
12 Kunjathoor VV, Wilson DL, LeBoeuf RC: Increased atherosclerosis in streptozotocin-induced diabetic mice. J Clin Invest 1996;97:1767–1773.
13 Lawrence WT, Diegelmann RF: Growth factors in wound healing. Clin Dermatol 1994;12:157–169.
14 Newman PJ, Berndt MC, Gorski J, White GCD, Lyman S, Paddock C, Muller WA: PECAM-1 (CD31) cloning and relation to adhesion molecules of the immunoglobulin gene superfamily. Science 1990;247:1219–1222.
15 Nilsson J, von Euler AM, Dalsgaard CJ: Stimulation of connective tissue cell growth by substance P and substance K. Nature 1985;315:61–63.
16 Pecoraro RE, Reiber GE, Burgess EM: Pathways to diabetic limb amputation. Basis for prevention. Diabetes Care 1990;13:513–521.
17 Reiber GE, Pecoraro RE, Koepsell TD: Risk factors for amputation in patients with diabetes mellitus. A case-control study. Ann Intern Med 1992;117:97–105.
18 Schatteman GC, Hanlon HD, Jiao C, Dodds SG, Christy BA: Blood-derived angioblasts accelerate blood-flow restoration in diabetic mice. J Clin Invest 2000;106:571–578.
19 Schratzberger P, Schratzberger G, Silver M, Curry C, Kearney M, Magner M, Alroy J, Adelman LS, Weinberg DH, Ropper AH, Isner JM: Favorable effect of VEGF gene transfer on ischemic peripheral neuropathy. Nat Med 2000;6:405–413.
20 Senapati A, Anand P, McGregor GP, Ghatei MA, Thompson RP, Bloom SR: Depletion of neuropeptides during wound healing in rat skin. Neurosci Lett 1986;71:101–105.
21 Servold SA: Growth factor impact on wound healing. Clin Podiatr Med Surg 1991;8:937–953.
22 Shi Q, Rafii S, Wu MH, Wijelath ES, Yu C, Ishida A, Fujita Y, Kothari S, Mohle R, Sauvage LR, Moore MA, Storb RF, Hammond WP: Evidence for circulating bone marrow-derived endothelial cells. Blood 1998;92:362–367.
23 Swift ME, Kleinman HK, DiPietro LA: Impaired wound repair and delayed angiogenesis in aged mice. Lab Invest 1999;79:1479–1487.